

Validity of the Rooted Staggered Determinant in the continuum limit

Anna Hasenfratz* and Roland Hoffmann†

Department of Physics, University of Colorado, Boulder, CO-80309-390

We investigate the continuum limit of the rooted staggered determinant in the 2-dimensional Schwinger model. We match both the unrooted and rooted staggered determinant with an overlap fermion determinant of two (one) flavors and a local pure gauge effective action by fitting the coefficients of the effective action and the mass of the overlap operator. The residue of this fit measures the difference of the staggered and overlap fermion actions. We show that this residue scales at least as $O(a^2)$, implying that any difference, be it local or non-local, between the staggered and overlap actions becomes irrelevant in the continuum limit. This observation justifies the rooting procedure.

I. INTRODUCTION

Staggered fermions offer many computational advantages over other fermion formulations. Simulations can be performed in large volumes at fairly small quark masses and data with improved actions show small scaling violations. However, the staggered action does not have full chiral symmetry and the chiral limit has to be taken together with the continuum limit. This is no different from other non-chiral actions, but staggered fermions have another, potentially serious problem. In 4 dimensions the staggered action describes four species (or tastes) of fermions, it cannot describe a single Dirac particle directly. In order to reduce the number of tastes from four to one the 4th root of the fermion determinant is taken in the path integral and there is no a priori reason that this rooted determinant corresponds to a local fermionic action belonging to the same universality class as 1-flavor QCD.

Several analytical and numerical works addressed this question in the last few years [1, 2, 3, 4, 5, 6, 7, 8, 9, 10]. None of them showed evidence that the procedure introduces non-universal errors, i.e. errors that cannot be considered cutoff effects that scale away in the continuum limit, but neither could they prove the validity of the rooting procedure. Recently it has been argued, based on a number of reasonable conjectures, that while the rooted staggered action is non-local at any finite lattice spacing, in the continuum limit the non-local terms become irrelevant [11, 12].

In this paper we present numerical evidence obtained in the 2-dimensional Schwinger model, showing that the rooted staggered action is in the right universality class. While the Schwinger model is much simpler than 4-dimensional QCD, its basic properties are QCD-like and therefore we believe that this work gives strong indication that the rooting procedure is safe and valid for 4-dimensional QCD simulations. We also show that the staggered action can be considered equivalent to a chiral Ginsparg-Wilson action only when the staggered mass is larger than typical taste symmetry breaking effects, limiting the parameter space where staggered simulations can be expected to approximate continuum QCD. We describe how the masses of the staggered and corresponding overlap actions should be matched to obtain physically equivalent theories when this condition is satisfied.

*Electronic address: anna@eotvos.colorado.edu

†Electronic address: hoffmann@pizero.colorado.edu

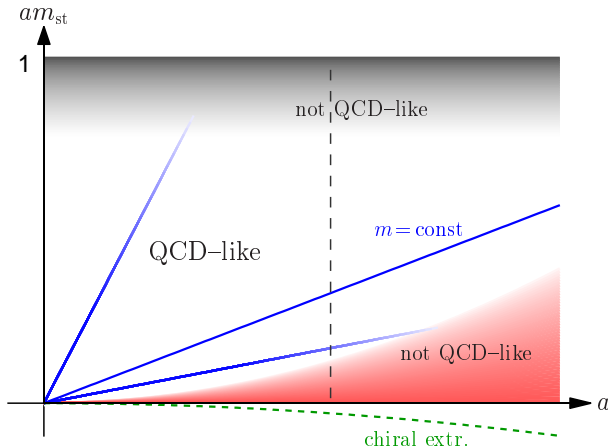


Figure 1: The expected phase diagram of the unrooted staggered action. The solid blue lines show how the continuum limit is approached with fixed physical mass. This approach should avoid the shaded regions dominated by cutoff effects or strong taste symmetry violation, respectively. Neither of those is expected to show QCD-like behavior.

II. THE CONTINUUM LIMIT OF THE STAGGERED ACTION

The partition function of the unrooted staggered action is

$$\begin{aligned} Z &= \int D[U \bar{\psi} \psi] e^{-S_g(U) - \bar{\psi}(M + am_{st})\psi} \\ &= \int D[U] \det(M + am_{st}) e^{-S_g(U)}, \end{aligned} \quad (1)$$

where $S_g(U)$ is a gauge action, M is the staggered Dirac operator and am_{st} is the bare staggered mass. The staggered action has two relevant couplings, a gauge coupling that determines the lattice spacing a and the fermion mass m_{st} . In the $a \rightarrow 0$ continuum limit the staggered action describes $n_t = 4$ degenerate fermions in 4, $n_t = 2$ fermions in 2 dimensions. At finite lattice spacing the taste symmetry is broken, the action describes n_t fermion tastes but only with a remnant $U(1)$ taste symmetry. The phase diagram in the relevant parameters a and am_{st} is sketched in Fig.1, where the solid blue lines illustrate how the continuum limit with fixed mass can be approached.

Fixed finite lattice spacing corresponds to a vertical line, like the dashed line in Fig.1. The latter can be divided into three regions:

- At $am_{st} = 0$ the staggered action's spectrum has a single Goldstone particle and $n_t^2 - 1$ massive pseudoscalars. While $n_t^2 - 2$ of these will become massless as $a \rightarrow 0$, at any finite lattice spacing the staggered spectrum is very different from n_t -flavor massless QCD. At small fermion mass $am_{st} \gtrsim 0$ the taste breaking terms dominate and the non-Goldstone pions are heavy compared to the Goldstone one. Again one does not expect QCD-like behavior.
- $am_{st} \gtrsim 1$ is the cutoff region (upper shaded area), again not continuum QCD-like.
- Only in the middle of the diagram, between the two shaded regions, would one expect to observe QCD. The $a \rightarrow 0$, $am_{st} \rightarrow 0$ continuum limit should be approached here.

While staggered fermions formally allow $am_{\text{st}} = 0$, physically this limit does not correspond to QCD at any finite lattice spacing [7, 8]. Simulations cannot be trusted at a small fermion mass where taste breaking terms dominate the pseudoscalar sector. However, the taste breaking terms are expected to scale at least with $O(a^2)$, such that at small enough lattice spacing the continuum limit can be approached with any finite fermion mass. Thus the exclusion of $am_{\text{st}} = 0$ is not a serious problem for massive fermions. We will discuss the case of massless fermions further at the end of Sect. IV.

The staggered determinant can always be written as

$$\det(M + am_{\text{st}}) = \det^{n_t}(D_{1\text{f}} + am_{1\text{f}}) \det(T), \quad (2)$$

where $D_{1\text{f}} + am_{1\text{f}}$ is an arbitrary 1-flavor Dirac operator and $\det(T)$ describes all the terms that are not included in the latter. If the local $D_{1\text{f}}$ operator and the mass term $m_{1\text{f}}$ could be chosen such that T contains only local gauge terms,

$$\det(T) = e^{-S_{\text{eff}}(U)}, \quad (3)$$

the staggered action would differ from an n_t -flavor degenerate Dirac operator only in cutoff level terms [2]. This is indeed the case for heavy, $am_{\text{st}} \gtrsim 1$ fermions, the upper shaded region in Fig.1.

On the other hand there are several examples that illustrate that at $am_{\text{st}} = 0$ the operator T cannot be local at any finite lattice spacing. In 4 dimensions the staggered theory has one massless Goldstone boson and 15 heavy pseudoscalars at vanishing bare quark mass. A theory with 4 degenerate flavors has either 15 massless Goldstone bosons if $am_{1\text{f}} = 0$ or none if $am_{1\text{f}} \neq 0$. None of these possibilities can match the spectrum of the staggered theory [11]. Similarly, on topologically non-trivial configurations a chiral $D_{1\text{f}}$ has an exact zero mode per topological charge, $\det^4(D_{1\text{f}} + am_{1\text{f}})$ vanishes as $am_{1\text{f}} \rightarrow 0$. The staggered operator does not have exact zero modes at finite lattice spacing and therefore the left hand side of Eq.(2) is finite even when $am_{\text{st}} = 0$. If $am_{\text{st}} = 0$ implies $am_{1\text{f}} = 0$, $\det(T)$ has to diverge, it cannot be identical to a local gauge operator at finite lattice spacing [10, 11] [16]. Numerical simulations of the finite temperature phase transition at zero fermion mass in 4 dimensions also indicate that the massless theory is not QCD-like [13], showing $O(2)$ rather than $O(4)$ critical exponents.

Recently Bernard et al. [11] argued that $\det(T)$ cannot be a local operator even at finite fermion mass at finite lattice spacing. This, however, does not mean that the staggered operator cannot describe QCD in the continuum limit. If we write the determinant as

$$\det(T) = e^{-S_{\text{eff}}(U)} \det(1 + \Delta), \quad (4)$$

and can choose S_{eff} such that the non-local term Δ is bounded at finite mass and goes to zero as $a \rightarrow 0$, the staggered determinant in Eq.(2) will describe n_t degenerate flavors in the continuum limit. This is certainly the expected behavior for the unrooted action.

Now we turn our attention to the rooting procedure. With the notation introduced above the root of the staggered determinant is

$$\det^{1/n_t}(M + am_{\text{st}}) = \det(D_{1\text{f}} + am_{1\text{f}}) e^{-S_{\text{eff}}(U)/n_t} \det^{1/n_t}(1 + \Delta). \quad (5)$$

If one could show that a

$$\Delta \rightarrow 0 \quad \text{as } a \rightarrow 0, \quad (6)$$

the rooted determinant of Eq.(5) would correspond to a local 1-flavor action in the continuum limit.

Based on renormalization group arguments, in Ref. [4] Shamir showed that this is indeed the case for free fermions. In a recent work [12], based on a number of reasonable assumptions, he argues that the same is true in the interacting theory.

Refs. [4, 12] describe an explicit method to find $D_{1f} + am_{1f}$ and the corresponding effective gauge action S_{eff} , but the construction is not unique. In fact, any Dirac operator and effective gauge action that satisfy Eqs.(5,6) will justify the rooting procedure. In the following we pick an arbitrary Ginsparg-Wilson operator as D_{1f} and ask if am_{1f} and $S_{\text{eff}}(U)$ can be chosen such that Eq.(6) is satisfied.

III. MATCHING THE FERMIONIC DETERMINANTS

The actual matching strategy is fairly general and we will describe it for an arbitrary pair of Dirac operators $D_1 + am_1$ and $D_2 + am_2$. We want to know to what extent the determinant of the first Dirac operator can be described by the determinant of the second plus pure gauge terms. To find this we calculate the determinant ratio

$$\det(T) = \frac{\det(D_1 + am_1)}{\det(D_2 + am_2)} \quad (7)$$

on a set of dynamical configurations generated at some given lattice spacing with the action

$$S_1 = S_g(U) + \bar{\psi}(D_1 + am_1)\psi. \quad (8)$$

Next we fit the logarithm of the determinant ratios with a pure gauge action of the form

$$S_{\text{eff}} = \sum_{l=0}^{l=n} \alpha_l \mathcal{C}_l(U), \quad (9)$$

where $\mathcal{C}_l(U)$ denotes traces of Wilson loops. The effective action S_{eff} has to be local, the coefficients α_l have to decay exponentially with the length of the loops. In practice we use an ultralocal effective action. The accuracy of the matching at fixed fermion mass m_2 is characterized by the per flavor/taste residue [17]

$$r(m_2) = \left\langle \left(\log \frac{\det(D_1 + am_1)}{\det(D_2 + am_2)} - S_{\text{eff}}(U) \right)^2 \right\rangle^{1/2}. \quad (10)$$

The minimum of the residue $r(m_2)$ in terms of m_2 determines the action $D_2 + am_2$ that is *physically closest* to the original $D_1 + am_1$ action. In this sense it defines the mass \bar{m}_2 that matches the fermion mass m_1 . In the notation of Eq.(4) then

$$r(\bar{m}_2) = \left\langle \left(\log \det(1 + \Delta) \right)^2 \right\rangle^{1/2}. \quad (11)$$

If the two fermion operators describe the same continuum theory the residue has to vanish as $a \rightarrow 0$ at fixed volume and quark mass.

IV. SCHWINGER MODEL - NUMERICAL RESULTS

A. Setup and matching tests

The 2-dimensional Schwinger model offers an excellent testing ground for the matching idea as it can be studied with high accuracy and limited computer resources. It is a super-renormalizable theory since the bare gauge coupling g is dimensional, the lattice gauge coupling is $\beta = 1/(ag)^2$. A continuum limit in fixed physical volume can be achieved by keeping the scaling variable $z = Lg$ fixed while increasing the lattice resolution. We choose $z = 6$ and vary the lattice size between $L/a = 12$ and $L/a = 28$ so the corresponding gauge coupling $\beta = (L/a)^2/z^2$ varies between 4 and ~ 22 , in or at least close to the the scaling regime. The scaling parameter z characterizes the (physical) volume while we use mL to fix the mass.

We produced gauge configurations using a global heatbath for the plaquette gauge action. The use of a global algorithm is essential to this study since at large values of β the autocorrelation time for topological charge fluctuations increases dramatically with both (local) heatbath and Metropolis. In fact, at the chosen physical volume these algorithms no longer tunnel between topological sectors at all for $\beta \gtrsim 10$ and thus in practice lose ergodicity.

In the data analysis, measurements on the pure gauge ensemble are reweighted with the appropriate power of the fermion determinant to obtain the observables in the full dynamical theory. On the gauge configurations we measure a set of Wilson loops \mathcal{C}_l as well as the complete spectra of the Dirac operators under consideration. For the matching we use an effective action (see Eq.9) that contains 9 loops up to length 10. With a maximal extension of four lattice units S_{eff} is very localized even on our coarsest lattices and in particular we do *not* increase the size or number of loops as we approach the continuum. Naturally, these Wilson loops are strongly correlated and in all cases a similar quality matching could be achieved using 3 appropriately chosen loops only. On the other hand, the matching does not improve significantly when using many more loops in the fit, indicating that Eq.(3) cannot be satisfied.

As a first test of our matching method, we compared a smeared overlap action to an unsmeared overlap action. Both actions have the same (plain Wilson) kernel but different Ginsparg-Wilson R_0 parameters. As expected in the case where both operators respect chiral symmetry, we see a linear relation between m_1 and the matching \overline{m}_2 for small quark masses and the residue $r(\overline{m}_2)$ is very small (3% at $\beta = 4$, decreasing to 0.2% on the finest lattice). Moreover, there is no observable dependence of $r(\overline{m}_2)$ on the fermion mass m_1 , which implies that the matching we attempt works equally well at all masses. Next we matched a Wilson Dirac operator with a smeared overlap action. We found that the residue is significantly larger (20% decreasing to 4%) but scales as expected when a is decreased. Also, by extrapolating the matched Wilson mass to vanishing overlap mass, we predict the critical mass am_c in excellent agreement with the large volume results of Ref. [14] that used the pion mass to identify am_c . This agreement shows that our matching procedure, while not based on physical observables, identifies the parameters where the two actions are physically closest.

In the following we concentrate on the matching of the staggered action. As a matching action we use a smeared overlap action with Ginsparg-Wilson radius $R_0 = 1$ and plain $r = 1$ Wilson kernel. The smearing is a single (projected) APE step with $\alpha = 0.4$ smearing parameter. The specific choice of the matching overlap action is not particularly important but we found better matching with the smeared link action. We have done exploratory studies with unsmeared overlap actions and with different R_0 choice but the results were not significantly different.

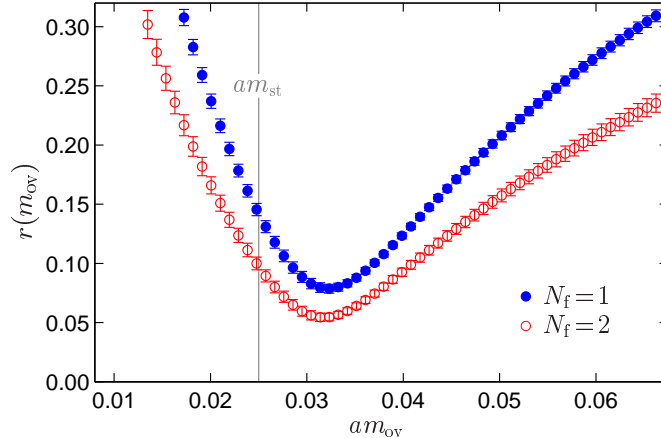


Figure 2: The residue of Eq.(10) as the function of the matching mass. The dynamical $L/a = 20$ configurations were generated with the staggered action at $am_{st} = 0.025$ and matched with an overlap action. Open red circles: 2 tastes/flavors; filled blue dots: 1 taste/ flavor.

B. The unrooted staggered action

We start our investigation with the unrooted action, which in 2 dimensions corresponds to two fermion tastes. In the continuum limit it is expected to describe two degenerate flavors and thus it should differ from a degenerate 2-flavor overlap action in irrelevant terms only. Our goal is to match the staggered determinant with a 2-flavor overlap action and local gauge terms at fixed physical mass and volume and study the residue of the matching (Eqs.10,11) as the lattice spacing $a \rightarrow 0$. Since we do not expect any strange behavior here, this section serves as an illustration and test of the matching procedure.

Fig.2 shows the matching of the $n_t = 2$ staggered determinant with the $N_f = 2$ flavor-degenerate overlap determinant at $z = 6$ on $L/a = 20$ lattices ($\beta \simeq 11.11$). The quenched configurations were reweighted to the dynamical staggered ensemble at $am_{st} = 0.025$. The residue of the matching (Eq.10) has a well defined minimum at $a\bar{m}_{ov} = 0.0317(3)$.

By repeating the matching at different values of the staggered masses am_{st} we can find the matching overlap masses at the given lattice spacing as shown by the blue dots in Fig.3a. For larger masses the data show a linear dependence with a constant offset, $\bar{m}_{ov} = 1.077(7)m_{st} + 0.0036(4)/a$. This kind of functional form was conjectured in Ref. [10]. For small masses, below $am_{st} \approx 0.02$, there is a clear deviation from the linear behavior. The residue of the fit also shows a rapid increase below this value (Fig.3b) indicating that the matching is no longer meaningful. According to the discussion in Sect.II we interpret this as the staggered action being QCD-like for $am_{st} \gtrsim 0.02$ and not QCD-like below.

As a consistency check we repeated the matching using the overlap action for the dynamical configurations and matching the overlap determinant with the staggered one. The result, shown by the red circles in Fig.3a, is the mirror image of the staggered with overlap matching data up to the point where the latter matching breaks down. This is the expected behavior if the two actions differ only by lattice artifacts. The agreement is even more obvious in Fig.4a where we replot the data of Fig.3a showing the difference of the matched staggered and overlap masses as the function of the overlap mass. The only difference between the two data sets in Fig.3 is the

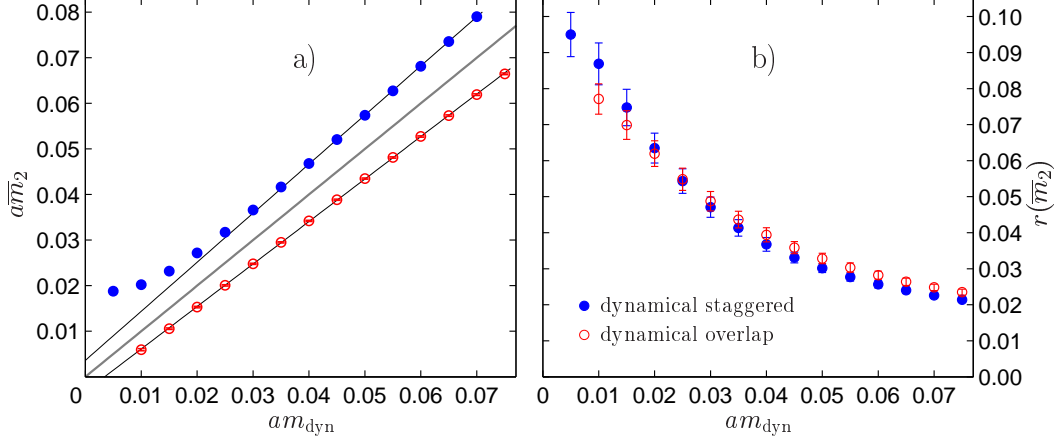


Figure 3: a) The matching mass as the function of the dynamical action mass at fixed lattice spacing for 2 tastes/flavors. Filled blue dots: staggered action matched with overlap; open red circles: overlap action matched with staggered. b) The residue of the matching described in a).

configuration ensemble used: staggered dynamical configurations for the staggered with overlap matching, dynamical overlap configurations for the overlap with staggered matching.

By restricting the configurations to the sector of trivial topology we could verify that the difference between the matching on the two ensembles and also most of the residue can be ascribed to configurations with non-vanishing topological charge. The massless overlap operator has a zero mode on these configurations while the smallest eigenvalue of the staggered operator is non-zero, determined by the taste breaking of the staggered action. Thus these configurations are not sufficiently suppressed at small quark masses in the staggered ensemble. Our matching procedure tries to compensate for this by assigning an even smaller quark mass until the matching breaks down entirely. This effect should become smaller when the number of flavors is reduced since the suppression of topology becomes weaker also for the overlap ensemble.

The shaded area in Fig.4 corresponds to the inaccessible region of $am_{\text{st}} < 0$. The overlap with staggered matching works basically up to this region. Extrapolating to the chiral limit of the overlap action suggests that the critical mass for staggered fermions is negative, $(am_{\text{st}})^{\text{cr}} = -0.0037(2)$ at these parameter values. Of course this is a non-physical value, well beyond the QCD like regime of staggered fermions. As argued above, the staggered with overlap matching breaks down at a much larger mass. Apparently configurations created with the staggered action at smaller mass values cannot be reasonably described by an overlap action, signaling the non QCD-like region of staggered fermions.

Next we consider the continuum limit of the matching at fixed physical mass [18] and volume $z = gL = 6$. Fig.5a shows the residue of matching the 2-taste staggered determinant with the 2-flavor overlap determinant at different masses as a function of a^2g^2 . The smaller the mass, the larger the matching residue is, as it is also evident from Fig.3b. For the smallest mass, $m_{\text{ov}}L = 0.4$ the data stops around $a^2g^2 = 0.11$ - on coarser lattices the two actions cannot be matched, the residue of Eq.(10) has no minimum. Nevertheless matching is possible at smaller lattice spacing and the residue at fixed $m_{\text{ov}}L$ approaches zero at least quadratically in a . The continuum limit can be approached with any fermion mass and the staggered determinant can be described as a 2-flavor chiral determinant plus pure gauge terms. This is the behavior we expected from universality.

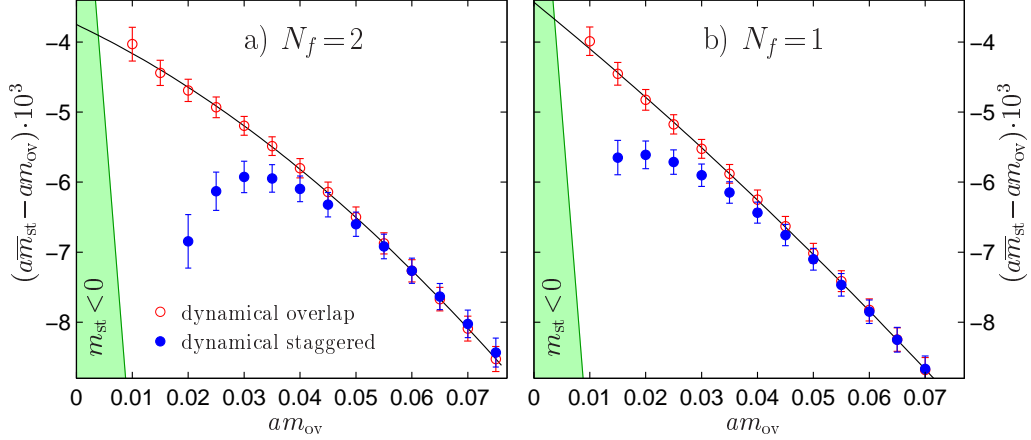


Figure 4: The difference of the matched staggered and overlap masses vs. the overlap mass at fixed lattice spacing. The notation is the same as in Fig.3. a) unrooted staggered/2-flavor overlap; b) rooted staggered/1-flavor overlap matching.

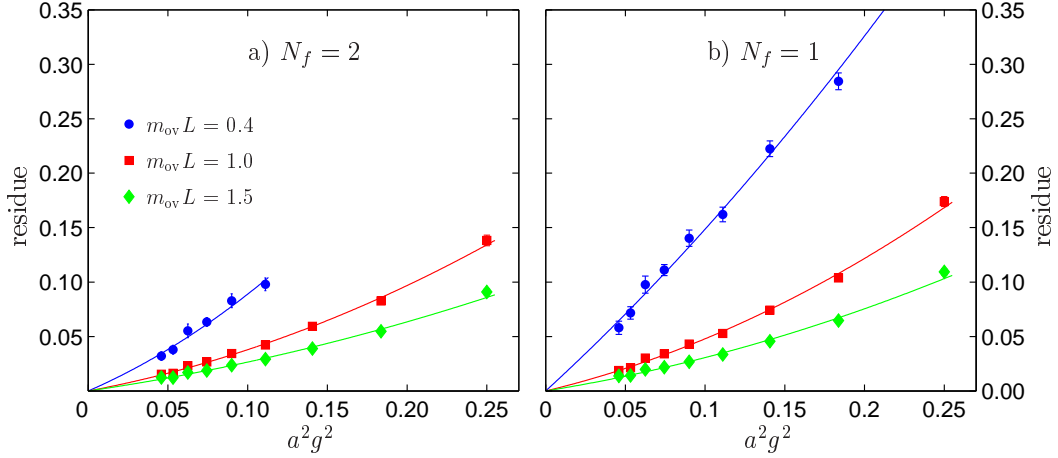


Figure 5: Residue of the matching as a function of the (squared) lattice spacing at different physical masses. a) unrooted staggered/2-flavor overlap; b) rooted staggered/1-flavor overlap matching.

C. The rooted staggered action

Now we repeat the analysis of the previous section for the rooted staggered action. The procedure is very similar. The pure gauge configurations are reweighted with the square root of the staggered determinant to generate configurations with one taste and the rooted determinant is matched with the 1-flavor overlap determinant plus pure gauge terms, according to Eq.(10).

The quality of the matching is very similar to the unrooted/2-flavor case as the open circles in Fig.2 show. In fact, even the matched mass $a\bar{m}_{ov} = 0.0322(2)$ hardly differs from the 2-flavor case. The 1-flavor data in Figs.3 is indistinguishable from the shown 2-flavor data. Fig.4b shows the mass difference for the rooted/1-flavor matching. The matching of the overlap determinant with staggered is almost the same as in the unrooted case and also the "critical" mass $(am_{st})^{cr} = -0.0034(2)$ is in agreement with the 2-flavor data. As expected, the opposite, i.e. the matching of the staggered determinant on staggered dynamical configurations, works in a larger mass range in

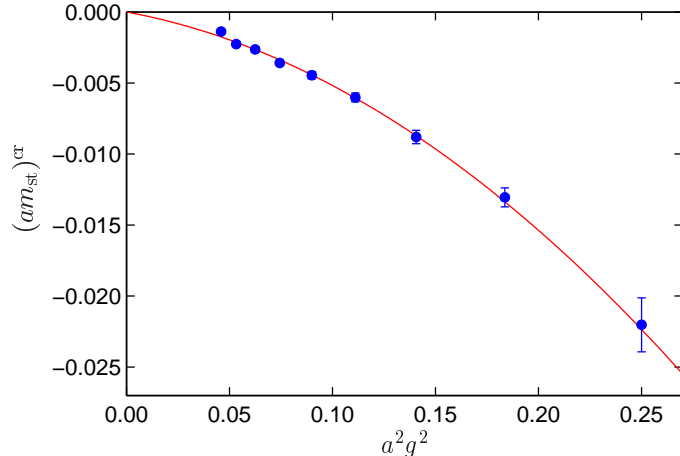


Figure 6: The staggered mass that corresponds to a chiral overlap action as the function of a^2 .

the rooted case.

Fig.5b is the important plot for the rooted staggered action as it shows the residue at fixed physical masses as the continuum limit is approached. There is a remarkable similarity between the 2- and 1-flavor cases. The residue for the 1-flavor rooted determinant is larger but the continuum approach is identical, at least quadratic in a . The taste violating term Δ in Eqs.(4) and (11) becomes irrelevant in the continuum limit. This result justifies the rooting procedure.

D. The phase diagram revisited

Our matching data can be used to quantify the phase diagram we sketched in Fig.1. We have already discussed the chiral extrapolation line, the staggered mass line that corresponds to the chiral limit of the overlap action. While this “critical mass” is not in the physically accessible region, it influences the relation between the matched staggered and overlap masses. Its value is important in mixed action simulations where an overlap valence quark action is used with configurations generated with staggered sea quarks. Obviously the deviation of this “critical mass” from zero is a lattice artifact and should vanish in the continuum limit. That is indeed the case as is shown in Fig.6, where we show $(am_{st})^{cr}$ from the 1-flavor data, which agrees with the unrooted one but has smaller errors since the matching works closer to the chiral limit (see above).

We can also map out the QCD-like and non QCD-like regions as indicated in Fig.1. While this is not a uniquely defined boundary, its meaning is yet quite clear. To quantify it we adopt a somewhat arbitrary but reasonable definition: we consider the matching between the staggered and overlap actions possible if the matching residue $r(\overline{m}_{ov})$ (per flavor) is smaller than some predetermined number. The shaded bands in Fig.7a correspond to residues between 6% and 10%. The darker blue region is for the rooted/1-flavor case, the overlapping lighter red band is the unrooted 2-flavor boundary. As expected, the 2-flavor band approaches zero at least quadratically (see below). The interesting thing is that the rooted 1-flavor data show an almost identical behavior, again signaling that in the continuum limit the rooted action is as good as the unrooted one.

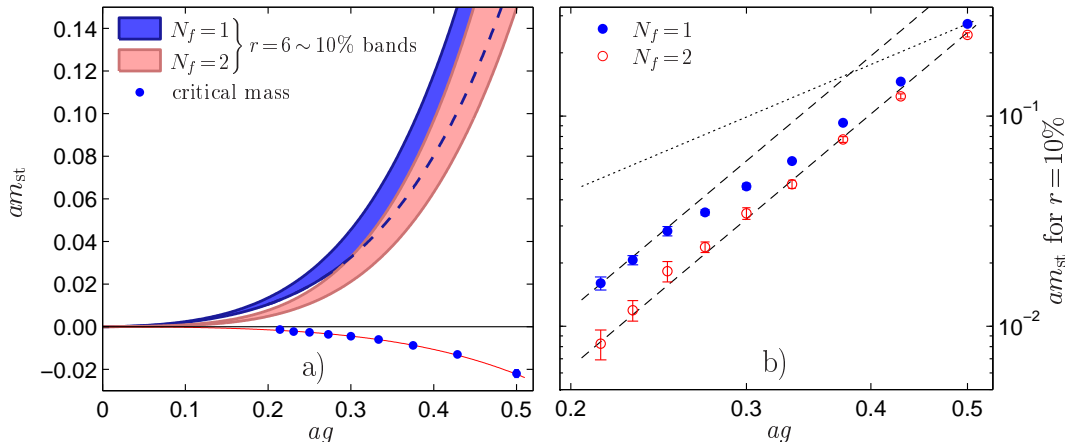


Figure 7: a) The phase diagram of the staggered action. The bands denote the regions where the matching residue is between 6 and 10%, indicating the onset of non QCD-like behavior. The data points at negative mass show where the staggered action would correspond to a chiral overlap action. b) Logarithmic plot of the staggered mass at 10% matching residue from part a).

E. Final comments

The data we presented in the previous sections correspond to thin link staggered fermions. Smearing link fermions have smaller taste breaking and show better scaling. When repeating the analysis with smeared staggered fermions, we found very similar behavior both for the rooted and for the unrooted case but indeed with greatly reduced taste breaking effects. In particular, at a given lattice spacing the matching worked down to much smaller quark masses. The lowest staggered eigenmode(s) on topologically non-trivial configurations are significantly smaller after smearing and thus the dynamical suppression of topology is much closer to that of a chiral overlap action.

Our data show that there is no problem with approaching the continuum limit at fixed physical mass (Fig.5). Whether massless fermions can be described in the continuum limit with the staggered action depends on the actual scaling of the taste violating terms. To achieve a chiral continuum limit the fixed point has to be approached at least like $am_{st} \propto a^2$, such that the physical mass $\sim \partial(am_{st})/\partial a$ vanishes in the $a \rightarrow 0$ limit. Since the mass shift in Fig.6 also disappears with $O(a^2)$, such a shift does not invalidate this argument. If the lines of constant residue in Fig.7a were quadratic, a staggered action with $am_{st} \propto a^2$ would have a constant deviation from a chiral overlap action *even in the continuum limit*. A chiral continuum limit thus requires that the staggered mass that corresponds to a constant matching residue vanishes faster than quadratically.

Fig.7b shows the mass at 10% matching residue in a logarithmic scale. The dashed lines are proportional to a^4 and while they describe the two-flavor data quite well, for the rooted action only the finest lattices are in agreement with a^4 scaling. However, in both cases the scaling is faster than quadratic (dotted line), thus making a chiral continuum limit possible. Note that this is the only place where we see a qualitative difference between the unrooted and rooted actions. The arguments from Sect.II offer a possible explanation. Since $\det(T)$ is non-local, on the coarser lattices this might affect our finite volume results, and only close to the continuum where the non-local terms become irrelevant does this finite volume effect go away. Apparently these non-local terms are more pronounced for the rooted action than for the unrooted one.

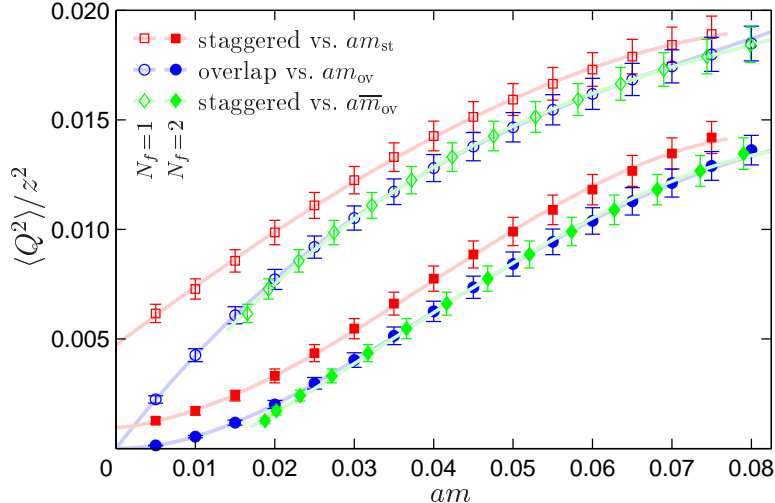


Figure 8: The topological susceptibility on the $L/a = 20$ ensemble. Open symbols refer to the one and filled symbols to the two flavor/taste results. After shifting the staggered data (red squares) to the matched overlap mass (green diamonds) almost perfect agreement with the overlap data (blue circles) is achieved.

Finally we illustrate the matching using a physical observable, the topological susceptibility $\langle Q^2 \rangle / z^2$, as this observable is very sensitive to the sea quarks. We define the topology through the zero-modes of the smeared overlap operator used in the matching and evaluate it on gauge ensembles generated with two and one flavor/taste staggered and overlap actions at various masses. Results from $L/a = 20$ lattices are shown in Fig.8, where the difference of the staggered and overlap ensemble at the same bare fermion mass is very evident, especially at small masses (red squares vs. blue circles). After shifting the staggered data to the matching overlap mass (green diamonds), excellent agreement is achieved. Again the one-flavor data shows better agreement since in the reweighting to two flavors any remnant mismatch in the weight becomes more important. The agreement on our finer lattices is equally good and extends to smaller quark masses. Fig.8 is similar to Fig.1 in Ref. [10] where matching between the staggered and overlap data was attempted by a constant mass shift. While a constant shift worked well for larger masses, it could not reproduce the small quark region. The shift presented in Fig.8 works everywhere but at the lightest mass.

V. CONCLUSION

The rooted staggered action is likely non-local in the physically relevant range of small quark masses. However, this does not invalidate the rooted action as long as the non-local terms are irrelevant and scale away in the continuum limit. Here we demonstrated that this is indeed the case in the 2-dimensional Schwinger model. We studied how the staggered action differs from a chiral overlap action along a line of constant physics as the continuum is approached. For both the unrooted (as expected) and rooted staggered action we found that the difference reduces to irrelevant local pure gauge terms. Nevertheless care is required in taking the continuum limit of staggered fermions such that the non QCD-like region is avoided.

It would be very interesting to repeat this calculation in 4 dimensions, where the determinant ratios would have to be calculated numerically. While difficult, it is not impossible to do that

using stochastic estimators and reduced determinants, especially in small volumes [15]. Whether the matching is reliable on small volumes could be studied within the Schwinger model first.

Acknowledgments

A.H. benefited from discussions and presentations of the unpublished works of Refs. [11, 12] during the "Workshop on the fourth root of the staggered fermion determinant" at the INT in Seattle and thanks the hospitality extended to her. We thank Y. Shamir for discussions that helped clarify several of the points made in this paper and also for a critical reading of the manuscript. We thank Ulli Wolff and the Computational Physics Group at the Humboldt University for the use of their computer resources. This research was partially supported by the US Dept. of Energy.

-
- [1] B. Bunk, M. Della Morte, K. Jansen, and F. Knechtli, Nucl. Phys. **B697**, 343 (2004), hep-lat/0403022.
 - [2] D. H. Adams (2004), hep-lat/0411030.
 - [3] F. Maresca and M. Peardon (2004), hep-lat/0411029.
 - [4] Y. Shamir, Phys. Rev. **D71**, 034509 (2005), hep-lat/0412014.
 - [5] S. Dürr and C. Hoelbling, Phys. Rev. **D69**, 034503 (2004), hep-lat/0311002.
 - [6] H. Neuberger, Phys. Rev. **D70**, 097504 (2004), hep-lat/0409144.
 - [7] S. Dürr and C. Hoelbling, Phys. Rev. **D71**, 054501 (2005), hep-lat/0411022.
 - [8] C. Bernard, Phys. Rev. **D71**, 094020 (2005), hep-lat/0412030.
 - [9] C. Bernard et al. (2005), hep-lat/0509176.
 - [10] A. Hasenfratz (2005), hep-lat/0511021.
 - [11] C. Bernard, M. Golterman, and Y. Shamir (2006), in preparation.
 - [12] Y. Shamir (2006), in preparation.
 - [13] J. B. Kogut and D. K. Sinclair (2006), hep-lat/0603021.
 - [14] N. Christian, K. Jansen, K. Nagai, and B. Pollakowski (2005), hep-lat/0510047.
 - [15] A. Hasenfratz, P. Hasenfratz, and F. Niedermayer, Phys. Rev. **D72**, 114508 (2005), hep-lat/0506024.
 - [16] The inconsistency of (2) on topologically non-trivial configurations was observed in Ref. [10]. In an attempt to keep the operator T local, Ref. [10] suggested a mass shift between the staggered and overlap actions. Based on the results presented here and in Ref. [11] we now conclude that T is non-local in the physically relevant regime even when allowing for a mass shift at finite lattice spacing.
 - [17] In the staggered case we use $(M + am_{st})^{1/n_t}$ at this point, which reduces the coefficients α_l and the residue r by a factor n_t , thus giving the per flavor residue.
 - [18] We fix the physical mass by keeping $m_{ov}L$ constant and vary the staggered sea quark mass to achieve the matching.